J|A|C|S
JOURNAL OF THE AMERICAN CHEMICAL SOCIETY

Communication
pubs.acs.org/JACS

α-Sulfur Crystals as a Visible-Light-Active Photocatalyst

Gang Liu,[†] Ping Niu,[†] Lichang Yin, and Hui-Ming Cheng*

Shenyang National Laboratory for Materials Science, Institute of Metal Research, Chinese Academy of Sciences, 72 Wenhua Road, Shenyang 110016, China

Supporting Information

ABSTRACT: We show that in contrast to conventional compound photocatalysts, α-sulfur crystals of cyclo-octasulfur (S_8) are a visible-light-active elemental photocatalyst. The α-S crystals were found to have the ability not only to generate ·OH radicals but also to split water in a photoelectrochemical process under both UV−vis and visible-light irradiation. Although the absolute activity obtained was low because of the large particle size and poor hydrophilicity of the α-S crystals studied, there is great potential for increasing the activity with the assistance of known strategies such as surface modification, nanoscaling, doping, and coupling with other photocatalysts.

Photocatalysis is an important process for converting solar energy to chemical energy.[1] One of the central missions that must be accomplished to enable its practical use in environmental and clean energy areas is finding efficient photocatalysts that operating well under solar light.[2−8] Ideal semiconductor photocatalysts should at least have the characteristics of absorbing visible light, suitable band edges for targeted reactions, good stability in water, environmental friendliness, and low cost. In the past decades, overwhelming attention has focused on compounds as photocatalysts, but the possible application of elemental semiconductors as photocatalysts has rarely been considered. Several elemental materials, including silicon, selenium, and red phosphorus, have not been demonstrated to be effective in decomposing azo dyes and photocatalytic hydrogen evolution from water splitting until recently.[9−11] These developments suggest that elemental semiconductors may represent a new class of photocatalysts for solar energy conversion.

Ionic sulfur is widely used in sulfide photocatalysts or as a dopant in oxide photocatalysts.[4,12] However, the possibility of using elemental sulfur as a photocatalyst has never been explored, to the best of our knowledge. Elemental sulfur has more than 30 allotropes, most of which consist of cyclic molecules with ring sizes of 6−20 sulfur atoms.[13,14] Among them, S_8 is the most stable configuration at standard temperature and pressure (STP) and can crystallize to form three solid allotropes: orthorhombic α-sulfur, monoclinic β-sulfur, and γ-sulfur. Orthorhombic α-S is the most stable form of sulfur at STP. The crownlike S_8 ring and the unit cell of α-S (a = 10.4646 Å, b = 12.8660 Å, c = 24.4860 Å) are shown in Figure 1a. Figure 1b gives the X-ray diffraction (XRD) pattern of the commercial α-S powder studied here. The α-S powder was amber-colored (Figure 1c inset), suggesting good absorption of visible light. The UV−vis absorption spectrum of α-S in Figure 1c shows intrinsic semiconductor-like absorption. The band gap of α-S determined from Figure 1c is 2.79 eV.

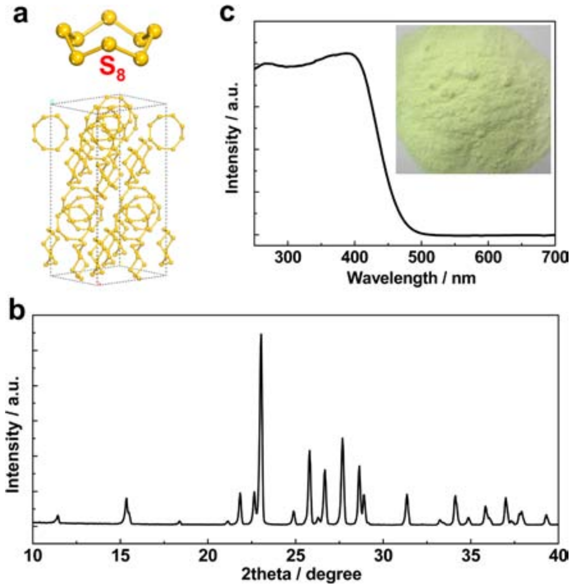

Figure 1. (a) Schematic illustration of the unit cell of an α-S crystal constructed from S_8 molecules. (b) Experimental XRD pattern of α-S crystal powder. (c) UV−vis absorption spectrum of α-S crystal powder. The inset in (c) is a photograph of the α-S crystal powder.

To understand the electronic structure of α-S, we conducted density functional theory (DFT) calculations. Figure 2a shows the calculated band structure of α-S with a direct band gap of 1.63 eV at the Γ point, which is 1.16 eV smaller than the experimental value (2.79 eV) as a result of the well-known band gap underestimation within the framework of standard DFT. Both the conduction and valence bands, consisting of major sulfur p orbitals and minor sulfur s orbitals, are moderately dispersed along all of the high-symmetry directions in the Brillouin zone. The wide valence band was also confirmed by the X-ray photoelectron spectroscopy (XPS) valence band spectrum of α-S (Figure S1 in the Supporting Information). The fluorescence emission spectrum recorded from α-S crystal powder (Figure 2b) shows a wide emission peak centered at ca. 502 nm, which corresponds to the direct band-to-band radiative recombination of photoexcited electrons and holes (the sharp

Received: March 25, 2012
Published: May 23, 2012

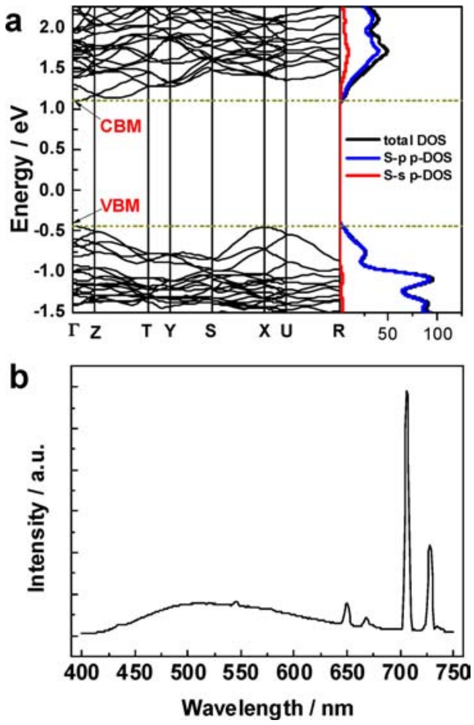

Figure 2. (a) Calculated (left) electronic band structures and (right) densities of states (DOS) for the unit cell of α-S crystals. CBM and VBM denote the conduction-band minimum and valence-band maximum, respectively. (b) Fluorescence emission spectrum of α-S crystals at room temperature. The excitation wavelength for fluorescence emission was 330 nm.

peaks that appear in Figure 2b are from Raman-active modes of α-S).

The energies of the valence-band maximum (VBM) and the conduction-band minimum (CBM) intrinsically determine the oxidation and reduction potentials of photoexcited holes and electrons in photocatalytic reactions. The VBM of α-S was determined to be 1.75 eV (Figure S1). This is 0.25 eV smaller than that of anatase TiO_2,[15] suggesting that α-S has a higher VBM than anatase TiO_2 by ca. 0.25 V relative to a normal hydrogen electrode (NHE). It has been established that the VBM of anatase TiO_2 is located at +2.64 V vs NHE at pH 7,[16] and the redox potentials for $\cdot OH/OH^-$ and $O_2/O_2^{\bullet -}$ were determined to be +1.9 and −0.33 V.[17,18] By comparison with the VBM of anatase TiO_2, the electronic potentials of the α-S crystals could be determined (Figure S2). Clearly, the oxidation potential of holes in α-S crystals is large enough to oxidize OH^- to $\cdot OH$.

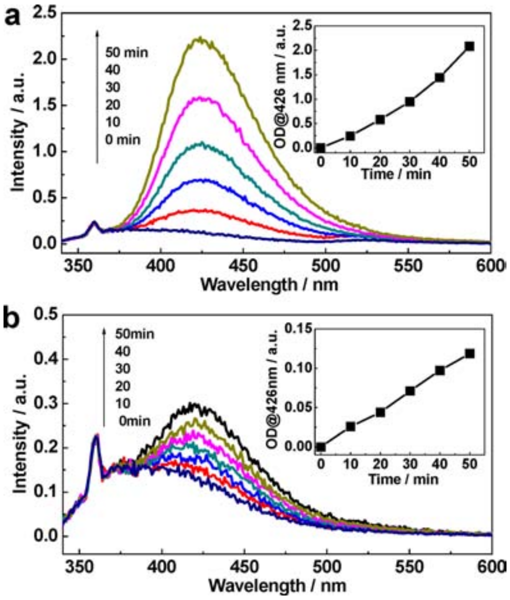

Figure 3. Time-dependent fluorescence emission spectra of TAOH formed by the reaction of TA with ·OH radicals generated by the α-sulfur photocatalyst under (a) UV−vis and (b) visible-light irradiation. The insets show the time-dependent fluorescence intensities of TAOH at 426 nm.

We next estimated the photocatalytic activity of α-S crystals in generating ·OH radicals using a method described previously.[15] It is known that ·OH reacts with terephthalic acid (TA) in basic solution to generate 2-hydroxyterephthalic acid (TAOH),[19] which emits a unique fluorescence signal with its peak centered at ca. 426 nm. As shown in Figure 3, significant fluorescent signals associated with TAOH were generated upon both UV−vis and visible-light irradiation of the α-S crystals suspended in a TA solution for different irradiation times. These results clearly suggest that the photoexcited holes in the valence band of the α-S crystals are powerful enough to oxidize surface-adsorbed hydroxyl groups and water to generate ·OH radicals. To confirm that ·OH radical generation proceeds through the photocatalysis process, the irradiation wavelength dependence of the fluorescence intensity at 426 nm due to TAOH generated with the α-S crystals was examined. As shown in Figure 4, the trend of TAOH generation was consistent with the UV−vis absorption spectrum of the α-S crystals, suggesting that the α-S crystals are photocatalytic active.

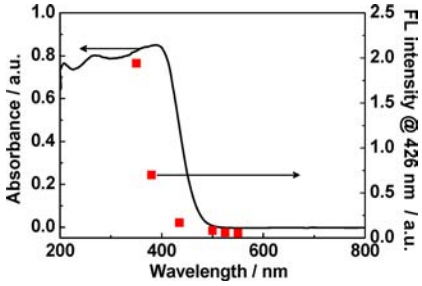

Figure 4. Irradiation wavelength dependence of the fluorescence intensity at 426 nm due to TAOH formed by the reaction of TA with ·OH radicals generated by the α-sulfur photocatalyst.

Moreover, the amount of ·OH radicals increased almost linearly with the irradiation time (Figure 3 insets), suggesting the stability of α-S crystals as photocatalysts. XRD, Raman, and XPS characterizations showed no detectable change in either the crystal structure of the α-S crystals or the chemical state of the sulfur. We further checked the concentration of sulfur-containing ions in the aqueous solution with suspended sulfur photocatalyst; no $S_2O_8^{2-}$ or S^{2-} was detected, and only a small amount of SO_4^{2-}/SO_3^{2-} (ca. 0.5 mg/L) was observed. Furthermore, the concentration did not increase with the irradiation time (Figure S3), suggesting that the α-S crystals act as a stable photocatalyst. For comparison, the stability of the widely investigated CdS photocatalyst was also examined. As shown in Figure S3, CdS suffered from serious photocorrosion. After 60 min of irradiation, the concentration of SO_4^{2-}/SO_3^{2-} in the aqueous solution with suspended CdS increased from

6.08 to 90.89 mg/L, which is 181 times higher than that from the α-sulfur suspended in aqueous solution.

On the basis of the relative positions of the VBM and CBM of α-S crystals, it was expected that the photoexcited electrons and holes in α-S would also have the ability to split water. To examine this expectation, we fabricated a photoanode of α-S crystals by electrophoretic deposition. This photoanode in a photoelectrochemical cell with a Na_2SO_4 solution as the electrolyte gave an apparent response to light on/off switching at the bias applied (Figure 5) under both UV−vis and visible-light irradiation. We analyzed the gaseous product from the photoelectrochemical cell after irradiation using a gas chromatograph. The obvious signal of H_2 was confirmed, suggesting that the α-S crystals do have the ability to split water. It is noted that the photocurrent density generated from the α-S photoanode is comparable to that from photoanodes of g-C_3N_4, a metal-free compound photocatalyst actively studied recently.[20,21]

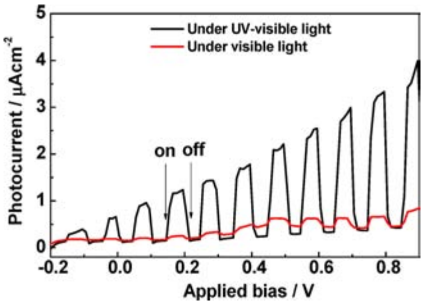

Figure 5. Applied potential bias dependence of the photocurrent generated by the photoanode of α-S crystals under UV−vis and visible-light irradiation.

Because of the large particle size (Figure S4A) and poor hydrophilicity of the α-S crystals studied, the photocatalytic activity demonstrated here is low. These drawbacks may be overcome by using common strategies for optimization of compound photocatalysts, such as nanoscaling, surface modification, doping, and coupling with other photocatalysts. As an initial attempt, we used a mechanical ball-milling process to decrease the particle size of the α-S crystals (Figure S4B). The milled crystals gave a substantially improved activity for decomposition of rhodamine B under both UV−vis and visible-light irradiation (Figure S5). It was found that the light absorption edge of sulfur powder after ball-milling was blue-shifted by ca. 25 nm as a result of quantum size effects (Figure S6), indicating an increase of 0.16 eV in the band gap and thus increased redox ability of photoexcited charge carriers in the milled sulfur. Increased redox ability of the carriers is beneficial for photocatalysis.[22,23] The activity improvement of the sulfur photocatalyst by ball-milling is therefore attributed to the synergistic effects of the decreased particle size and the increased redox ability of the charge carriers. In addition, the sulfur powder was suspended only on the surface of the aqueous solution as a result of its poor hydrophilicity, making it easy to separate from the solution. This could also be a merit of sulfur as a photocatalyst for the decomposition of pollutants in solution in terms of recycling of the photocatalyst.

In summary, we have shown the possibility of using α-S crystals in photocatalytic solar energy conversion. It has been demonstrated that the crystals indeed have the ability to generate important active species such as ·OH radicals for decomposing organic molecules and to split water under both UV−vis and visible-light irradiation. We expect elemental sulfur to provide new opportunities for the development of efficient visible-light-responsive photocatalysts.

■ ASSOCIATED CONTENT

Ⓢ Supporting Information

Detailed characterization, theoretical calculations, photocatalytic activity measurements, and Figures S1−S5. This material is available free of charge via the Internet at http://pubs.acs.org.

■ AUTHOR INFORMATION

Corresponding Author

cheng@imr.ac.cn

Author Contributions

†G.L. and P.N. contributed equally.

Notes

The authors declare no competing financial interest.

■ ACKNOWLEDGMENTS

The authors acknowledge Mr. Guolong Zang, Dr. Guoping Sheng, and Prof. Hanqing Yu (University of Science and Technology of China) for their help in determining the concentration of SO_4^{2-}/SO_3^{2-} in aqueous solution and thank the Major Basic Research Program, Ministry of Science and Technology of China (2009CB220001), the NSFC (50921004, 51002160, 21090343, and 51172243), the Solar Energy Initiative of the Chinese Academy of Sciences (CAS), and the Hydrogen Energy Program of CAS (KJCX2-YW-H21-01) for financial support. G.L. is grateful for the IMR SYNL-T.S. Kê Research Fellowship.

■ REFERENCES

(1) Fujishima, A.; Honda, K. *Nature* **1972**, *238*, 37.

(2) Hoffmann, M. R.; Martin, S. T.; Choi, W.; Bahnemann, D. W. *Chem. Rev.* **1995**, *95*, 69.

(3) Linsebigler, A. L.; Lu, G. Q.; Yates, J. T., Jr. *Chem. Rev.* **1995**, *95*, 735.

(4) Chen, X. B.; Shen, S. H.; Guo, L. J.; Mao, S. S. *Chem. Rev.* **2010**, *110*, 6503.

(5) Liu, G.; Wang, L. Z.; Yang, H. G.; Cheng, H. M.; Lu, G. Q. *J. Mater. Chem.* **2010**, *20*, 831.

(6) Maeda, K.; Teramura, K.; Lu, D. L.; Takata, T.; Saito, N.; Inoue, Y.; Domen, K. *Nature* **2006**, *440*, 295.

(7) Tada, H.; Kiyonaga, T.; Naya, S. *Chem. Soc. Rev.* **2009**, *38*, 1849.

(8) Zou, Z. G.; Ye, J. H.; Sayama, K.; Arakawa, H. *Nature* **2001**, *414*, 625.

(9) Kang, Z. H.; Tsang, C. H. A.; Wong, N. B.; Zhang, Z. D.; Lee, S. T. *J. Am. Chem. Soc.* **2007**, *129*, 12090.

(10) Chiou, Y. D.; Hsu, Y. J. *Appl. Catal., B* **2011**, *105*, 211.

(11) Wang, F.; Ng, W. K. H.; Yu, J. C.; Zhu, H. J.; Li, C. H.; Zhang, L.; Liu, Z. F.; Li, Q. *Appl. Catal., B* **2012**, *111−112*, 409.

(12) Yan, H. J.; Yang, J. H.; Ma, G. J.; Wu, G. P.; Zong, X.; Lei, Z. B.; Shi, J. Y.; Li, C. *J. Catal.* **2009**, *266*, 165.

(13) Steudel, R.; Eckert, B. *Top. Curr. Chem.* **2003**, *230*, 1.

(14) Meyer, B. *Chem. Rev.* **1964**, *64*, 429.

(15) Liu, G.; Wang, L. Z.; Sun, C. H.; Yan, X. X.; Wang, X. W.; Chen, Z. G.; Smith, S. C.; Cheng, H. M.; Lu, G. Q. *Chem. Mater.* **2009**, *21*, 1266.

(16) Sakthivel, S.; Kisch, H. *ChemPhysChem.* **2003**, *4*, 487.

(17) Mrowetz, M.; Balcerski, W.; Colussi, A. J.; Hoffmann, M. R. *J. Phys. Chem. B* **2004**, *108*, 17269.

(18) Bahnemann, D. W.; Hilgendorff, M.; Memming, R. *J. Phys. Chem. B* **1997**, *101*, 4265.

(19) Hirakawa, T.; Nosaka, Y. *Langmuir* **2002**, *18*, 3247.

(20) Wang, X. C.; Maeda, K.; Thomas, A.; Takanabe, K.; Xin, G.; Carlsson, J. M.; Domen, K.; Antonietti, M. *Nat. Mater.* **2009**, *8*, 76.

(21) Wang, Y.; Wang, X. C.; Markus, A. *Angew. Chem., Int. Ed.* **2012**, *51*, 68.

(22) Liu, G.; Niu, P.; Wang, L. Z.; Lu, G. Q.; Cheng, H. M. *Catal. Sci. Technol.* **2011**, *1*, 222.

(23) Holmes, M. A.; Townsend, T. K.; Osterloh, F. E. *Chem. Commun.* **2012**, *48*, 371.